JACS
JOURNAL OF THE AMERICAN CHEMICAL SOCIETY

Article

pubs.acs.org/JACS

Structure Revision of Plakotenin Based on Computational Investigation of Transition States and Spectroscopic Properties

Angela Bihlmeier,*[,†] Emmanuel Bourcet,[‡] Stephanie Arzt,[‡] Thierry Muller,[‡] Stefan Bräse,[‡] and Wim Klopper*[,†]

[†]Institute of Physical Chemistry, and [‡]Institute of Organic Chemistry, Karlsruhe Institute of Technology (KIT), Kaiserstrasse 12, 76131 Karlsruhe, Germany

Supporting Information

ABSTRACT: We show that the previously [*Tetrahedron Lett.* **1992**, *33*, 2579] proposed structure of natural plakotenin must be revised. Recently, the total synthesis of plakotenin was achieved via an intramolecular Diels–Alder reaction from a (*E*,*E*,*Z*,*E*)-tetraene as linear precursor. Using density functional theory, the computation of the four possible transition states for this reaction shows that the previously proposed structure could only have been formed via an energetically high-lying transition state, which is very unlikely. Instead, we suggest that the structure of plakotenin corresponds to the product formed via the lowest transition state. A comparison of experimental and theoretical optical rotation, circular dichroism, and two-dimensional nuclear Overhauser enhancement spectra conclusively proves that the structure of plakotenin is the one that is suggested by the transition state computations. Moreover, the simulation of the nuclear Overhauser enhancement spectra suggests that it is most likely that the misassignment of the ^{1}H chemical shifts of two methyl groups has led to the wrong structure prediction in the 1992 work. The previously proposed structure of *iso*-plakotenin remains unaffected by our structure revision, but the structures of *homo*- and *nor*-plakotenin must also be revised. The present work shows how the total synthesis of a natural product, together with the theoretical determination of the barrier heights of the reactions involved, can be of great help to assign its structure. It appears that intramolecular Diels–Alder reactions can be modeled accurately by today's first-principles methods of quantum chemistry.

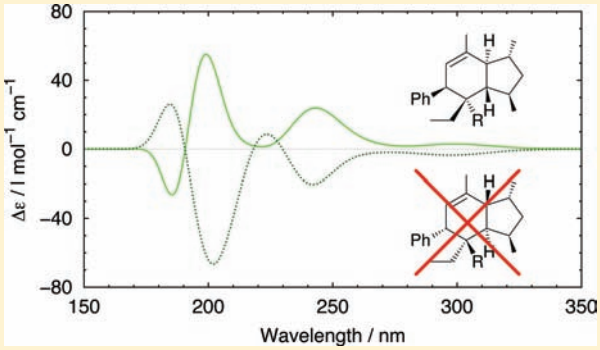

INTRODUCTION

Plakotenin (previously proposed structure **1***, Figure 1) is a secondary metabolite of polyketide origin, which was isolated for the first time in 1992 from an Okinawan marine sponge of the genus *Plakortis*.[1] In biological activity studies, plakotenin exhibited in vitro cytotoxicity against murine lymphoma L1210 and human epidermoid carcinoma KB cells.[1] Furthermore, it was shown that plakotenin significantly reduces proliferation of rheumatoid synovial fibroblasts.[2] The direct use of natural plakotenin for therapy is problematic, however, due to the very low availability of the marine organisms and the isolation of only very small amounts of the biologically active substance from the natural material. Thus, the efficient total synthesis of plakotenin is highly desirable.

On the basis of the original structure assignment, it was proposed that plakotenin might be biosynthetically derived from a linear precursor through an intramolecular Diels–Alder (IMDA) reaction.[1] The retrosynthetic analysis of the natural product yields a (*E*,*E*,*Z*,*E*)-tetraene as biosynthetic precursor (see Figure 1). The Diels–Alder reaction of the linear precursor is a key step in the total synthesis as it generates the required carbon framework and stereogenic centers. Recently, an analogous approach was successfully used in the total synthesis of spiculoic acid A,[3−7] a cytotoxic polyketide from the Caribbean marine sponge *Plakortis angulospiculatus*.[8] In contrast to spiculoic acid A whose biosynthetic precursor contains a trien–ene system, a diene–diene system is required for the synthesis of plakotenin. A closer look reveals that the tetraene may undergo four distinct intramolecular Diels–Alder reactions which lead to four distinct products, only one of which is plakotenin. The same is true for the analogue (*E*,*E*,*E*,*E*)-tetraene which can be used to access diastereomers of plakotenin.

In the present work, we try to understand the stereoselectivity of the intramolecular Diels–Alder reactions for both the (*E*,*E*,*Z*,*E*)- and (*E*,*E*,*E*,*E*)-tetraenes by computational studies of the respective transition states. While we find perfect agreement for the predicted lowest transition state of the (*E*,*E*,*E*,*E*)-tetraene and the proposed structure for the synthesized product *iso*-plakotenin (**2**, Figure 1), the transition state for the proposed structure (**1***) of the synthesized plakotenin molecule is predicted to be highest in energy. This is very suspicious since the transition states for both precursors

Received: September 15, 2011
Published: December 22, 2011

dx.doi.org/10.1021/ja2087097 | *J. Am. Chem.Soc.* 2012, 134, 2154–2160

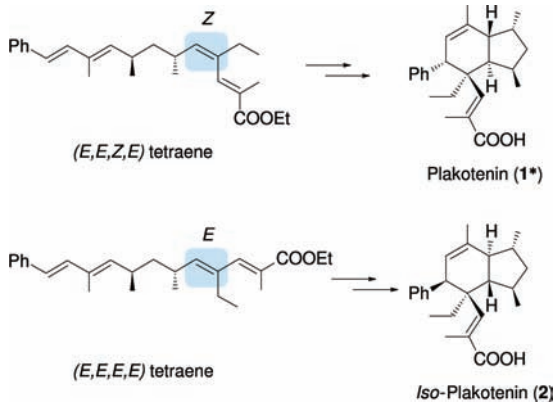

Figure 1. Schematic representation of the key step in the total synthesis of plakotenin (**1**) and *iso*-plakotenin (**2**). The final products are obtained after saponification of the IMDA cycloadducts. The structures presented in this figure were suggested in earlier work.[1,9] We show in the present work that the structure of plakotenin has to be revised. This revised structure will be denoted as **1**.

are very similar and the quality of the theoretical predictions should be equally good. As the synthesized compound obtained from the (*E,E,Z,E*) precursor indeed agrees with the natural product in all available spectroscopic data, doubts regarding the proposed stereochemistry of natural plakotenin arise.

We therefore carefully study the spectroscopic properties that allow the distinction of the two product structures in question, that is electronic circular dichroism (CD), optical rotation (OR), and two-dimensional nuclear Overhauser enhancement (2D-NMR). The results consistently show that the structure of natural plakotenin has to be revised.

SYNTHESIS OF PLAKOTENIN (1) AND *ISO*-PLAKOTENIN (2)

The total synthesis of plakotenin has been described in detail in previous work.[9] The required (*E,E,Z,E*) precursor was synthesized starting from commercially available enantiopure reagents in order to ensure the correct absolute stereochemistry of the Me groups. From the cycloaddition of the tetraene, a single diastereoisomer was obtained which after saponification yielded synthetic plakotenin. Its stereochemistry was deduced by extensive analysis of the 2D-NMR spectra. The spectroscopic data (^{1}H NMR, 2D-NOESY correlations) as well as the optical rotation of synthetic plakotenin were identical with the reported data of the natural product. On the basis of these results, it was concluded in ref 9 that the structure derived for the synthesized compound was in agreement with the previously assigned structure (**1***) for plakotenin.

In the case of *iso*-plakotenin, the (*E,E,E,E*) precursor was required. For this, the minor *E* isomer was separated from the major *Z* isomer after introduction of the third double bond, and the synthesis was completed analogously to the method described for plakotenin. Interestingly, the IMDA reaction of the all (*E*) configured linear precursor proceeded with less selectivity, since a 6.6:1 ratio of unseparable diastereoisomers could be determined by analysis of the ^{1}H NMR spectrum. Unfortunately, the relative stereochemistry of the minor diastereoisomer could not be determined, since the corresponding carboxylic acid could not be isolated. The stereochemistry of the main product was deduced by extensive analysis of the 2D-NMR spectra and assigned to be *iso*-plakotenin (**2**).

COMPUTATIONAL STUDIES AND DISCUSSION

In this section we present the results of our quantum chemical investigations and compare them with the data obtained for the synthesized compounds.

Transition States of the IMDA Reaction. The key step in the total synthesis of plakotenin (**1**) and *iso*-plakotenin (**2**) is the intramolecular Diels–Alder reaction of the respective tetraene precursor (Figure 1). Saponification of the resulting cyclic ethyl ester yields the desired carboxylic acid.

However, the precursor molecule may undergo not only one but four intramolecular Diels–Alder reactions involving different transition states and products. This is illustrated in Figure 2 for the (*E,E,Z,E*) precursor. The stereoselectivity of the intramolecular Diels–Alder reaction plays an important role in view of the development of high yield synthetic methods for

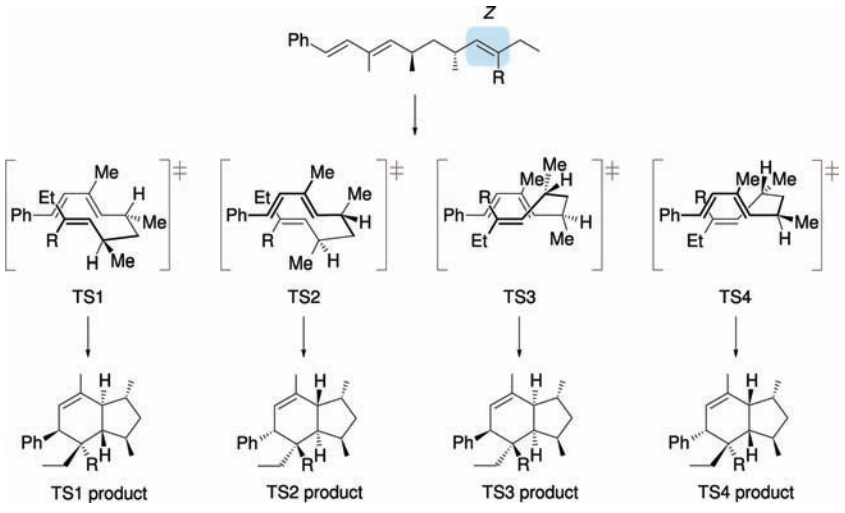

Figure 2. Possible transition states (shown as triene conformers) and products for the intramolecular Diels–Alder reaction of the (*E,E,Z,E*) precursor (R = $-$CH=CCH$_3$COOEt). The previously proposed structure (**1***) for natural plakotenin corresponds to the saponified product derived from TS2 (R = $-$CH=CCH$_3$COOH). In the present work, we show that the correct structure (**1**) derives from TS1. In the case of the (*E,E,E,E*) precursor, the R and Et groups are interchanged.

dx.doi.org/10.1021/ja2087097 | *J. Am. Chem.Soc.* 2012, 134, 2154–2160

plakotenin. We therefore wish to understand the product distribution on the basis of quantum chemical calculations. For this, we optimize the various transition states (TS1, TS2, TS3, and TS4) for both the (*E,E,E,E*)- and (*E,E,Z,E*)-tetraene precursor. In all cases, the geometries of the transition states indicate a strongly asynchronous reaction process with substantially different bond lengths r_1 and r_2 (Figure 3). The

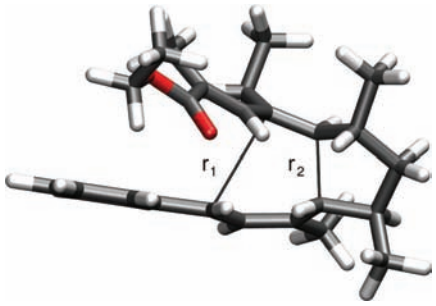

Figure 3. Optimized transition state for the intramolecular Diels–Alder reaction of the (*E,E,Z,E*) precursor. The lowest-energy conformer for TS1 is shown.

C–C bond distances as well as the relative energies of the lowest-energy conformer of each transition state are summarized in Table 1.

Table 1. Relative Energies of the Various Transition States (in kJ mol^{-1}) and C–C Bond Length of the Bonds Formed in the Course of the Diels–Alder Reaction (in pm)[a]

	ΔE	r_1	r_2
(*E,E,E,E*)			
TS1	0	296.2	191.8
TS2	46	288.9	187.7
TS3	32	288.7	191.7
TS4	20	295.4	189.4
(*E,E,Z,E*)			
TS1	0	303.1	190.7
TS2	43	305.6	191.7
TS3	36	281.7	197.9
TS4	28	285.2	192.2

[a]The absolute barrier height of the lowest transition state is 125 kJ mol^{-1} for (*E,E,E,E*) and 116 kJ mol^{-1} for (*E,E,Z,E*).

We find that the trends in the relative energies of TS1–TS4 are very similar for both precursor molecules. TS1 is the energetically most favored transition state, followed by TS4 and TS3. TS2 on the other hand is least favored and about 40 kJ mol^{-1} higher in energy. The distance r_2 amounts to approximately 190 pm, while the distance r_1 is substantially longer due to steric hindrance occurring between the substituents of the diene (Ph) and dienophile (Et and R). Given the relative transition state energies of both tetraenes, we assume that the influence of the configuration of the stereochemically relevant double bond (*E* or *Z*) is negligible. Overall, the results from the quantum chemical calculations appear plausible and suggest that the main product of the IMDA reaction of the (*E,E,E,E*) and (*E,E,Z,E*) precursor is formed via TS1.

Comparison of our transition state calculations with the experimental results reveals that the synthesized compound (**2**) starting from the (*E,E,E,E*)-tetraene is in agreement with the prediction that the IMDA reaction mainly proceeds via TS1. Concerning the minor product, one could speculate that it is derived from TS4 which is the second lowest transition state. In the case of the (*E,E,Z,E*)-tetraene, however, we find that the computational and experimental results are mutually inconsistent. While the reaction is predicted to occur via TS1, the structure determined in the experiment (**1***) belonged to TS2. This is even more peculiar as the contradiction is related to the natural product. On one hand we are convinced that the quantum chemical results are of comparable quality for both reactions, but on the other hand we are certain that the obtained products are plakotenin and *iso*-plakotenin. A resolution of the discrepancy seems impossible at this stage, and first doubts regarding the proposed structure for plakotenin emerge. We shall therefore study the spectroscopy of the products of TS1 and TS2 in the following section.

Products of TS1 and TS2: Conformational Isomers. The main objective of the investigation of product structures is the identification of characteristics that allow a clear-cut discrimination between the products of TS1 and TS2. Upon closer examination we notice that significant parts of the structures in question, namely the cyclohexene substructures, are in an enantiomeric relationship (see Figure 4). The only

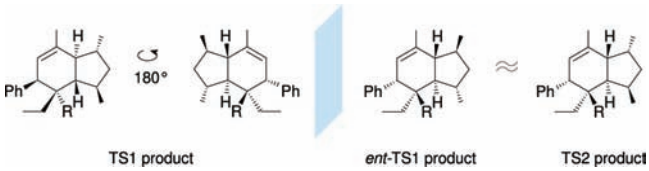

Figure 4. Products of the (*E,E,Z,E*)-tetraene derived from TS1 (left) and TS2 (right). Except for the Me groups situated at the five-membered ring, the structures are enantiomers.

difference arises from the stereochemistry of the two Me groups which are attached to the five-membered ring. This means that chiroptical properties, such as circular dichroism and optical rotation, should be well suited to distinguish between the given structures.

However, the flexibility of the product molecules makes the computational treatment difficult. Changes in the conformation may influence the properties we are interested in and therefore have to be accounted for. The main sources of flexibility are given by rotations about single bonds and various conformations of the fused rings. In order to generate a representative selection of conformers, we systematically search for minimum structures by considering rotations about the Et, –CH=CH_3COOH, and –COOH groups and two conformations for the five-membered ring (–CH_2– up/down) as well as for the six-membered ring (chair/boat). Following this strategy, we are able to locate 46 and 30 conformational isomers for the TS1 and TS2 products of the (*E,E,E,E*) precursor and 44 (TS1) and 38 (TS2) product conformers for the (*E,E,Z,E*) precursor.

Final CD spectra and values for the optical rotation are obtained by weighting the contribution of each conformer according to a Boltzmann distribution.

Chiroptical Properties. The computed CD spectra for the products of the (*E*) and (*Z*) configured tetraenes are displayed in Figures 5 and 6, respectively. As expected for structures of which the most relevant parts are in an enantiomeric relationship, we observe that the spectra of the TS1 and TS2 products are essentially identical but mirror-reversed with respect to the *x* axis. Moreover, the similarity of product spectra

dx.doi.org/10.1021/ja2087097 | J. Am. Chem.Soc. 2012, 134, 2154–2160

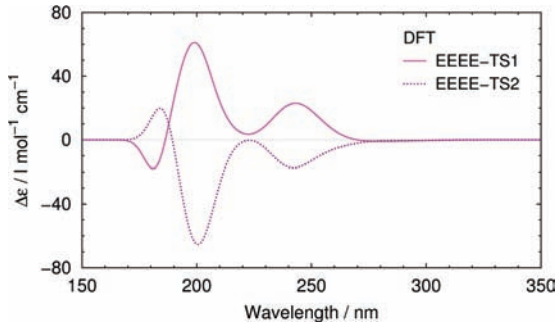

Figure 5. Simulated CD spectra for the products of (*E,E,E,E*)-TS1 and (*E,E,E,E*)-TS2.

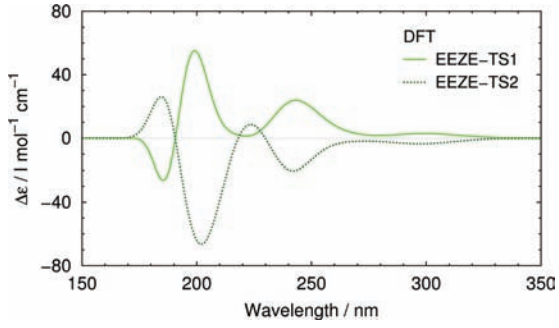

Figure 6. Simulated CD spectra for the products of (*E,E,Z,E*)-TS1 and (*E,E,Z,E*)-TS2.

that belong to the same transition state (for example, (*E,E,E,E*)-TS1 and (*E,E,Z,E*)-TS1) suggests that interchanging the Et and $-CH{=}CH_3COOH$ groups has only little effect on the absorption difference, $\Delta\varepsilon$. All obtained spectra basically exhibit two strong bands with peaks located at around 200 and 242 nm. In the case of the (*E,E,Z,E*) products, a further but comparatively weak signal is found at 300 nm. Note that our calculated excitation energies cover the range up to 185 nm which causes the spectra to reach zero level for lower wavelengths. Spectral features below 185 nm are therefore meaningless. The computed values for the optical rotation are listed in Table 2. Again, we observe similar results for the

Table 2. Computed and Measured Optical Rotation of the Products from (*E,E,E,E*) and (*E,E,Z,E*) Precursors (in deg dm^{-1} g^{-1} cm^3)

$[\alpha]_D^{20}$	TS1	TS2	Exp.
(*E,E,E,E*)	+267.6	−311.6	+184.6
(*E,E,Z,E*)	+270.0	−337.9	+193.0

products of the same transition state type. The optical rotations for structures derived from TS1 have the opposite sign compared to those for structures derived from TS2, with the absolute values being slightly larger in the case of TS2.

The measured CD spectra for our isolated products are shown in Figure 7. First of all, we notice that the data for plakotenin and *iso*-plakotenin are very similar. Both spectra show pronounced maxima at around 194 and 225 nm. In addition, a very weak and broad feature at 294 nm is detected for plakotenin. The measured values for the optical rotation are quoted in Table 2.

Given the computational results, the assignment of the synthesized compounds is unambiguous. The CD spectra as

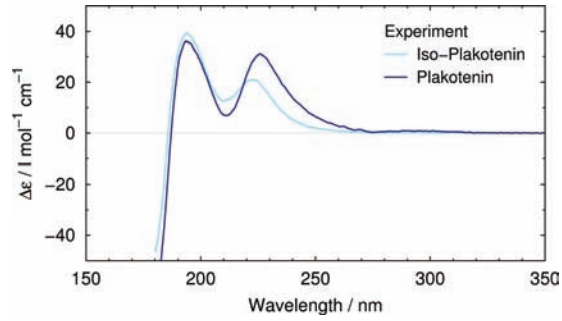

Figure 7. Measured CD spectra for the products obtained from the (*E,E,E,E*) and (*E,E,Z,E*) precursors after cycloaddition and saponification.

well as the optical rotation indicate that both structures are derived from IMDA reactions via transition state TS1. This is also in agreement with the calculated barrier heights. Hence, the structure which had previously been assigned to the product of the (*E,E,Z,E*) precursor was wrong. Comparison of our results with the chiroptical data reported for natural plakotenin (CD: λ_{ext} 226 nm ($\Delta\varepsilon$ +32); $[\alpha]_D^{19}$ +204°)[1] nevertheless reveals that the synthesized product is plakotenin! Thus, the structure proposed in 1992 for the natural product must be wrong.

Although the data presented so far are more than enough evidence to revise the structure of plakotenin, we are wondering about the original structure assignment based on 2D-NMR data. Here, two correlations had been observed[1] that in fact only fit to the wrong structure, and we shall elucidate this issue in the next section.

Two-Dimensional NMR Spectra. Two-dimensional nuclear Overhauser enhancement spectroscopy constitutes a useful tool to study the stereochemistry and conformation of molecules. It relies on spin relaxation processes via dipolar coupling which interacts through space and is thus able to detect protons that are in close proximity. The two structures we are interested in, that is the originally proposed (**1***) and our revised structure (**1**) of plakotenin, vary in the absolute configuration of all stereogenic centers in the cyclohexene subsystem. The Me groups which are attached to the five-membered ring therefore face a different chemical environment, and we expect corresponding differences for the NOESY correlations in the 2D-NMR spectra. Our aim therefore is to simulate the spectra for both structures in order to ensure that the results agree with the structure revision of plakotenin and in order to understand why the 1992 assignment failed.

Just as for the CD spectra and the optical rotation we take the Boltzmann average for the respective conformational isomers. We are aware that our data are generated on the basis of local minimum structures, which means that some signals in the 2D-NMR spectrum might be missing. This may happen when some protons occasionally get much closer, for example during movement over a rotation barrier. However, the more important point is that strong signals occurring in our simulation definitely must also be present in the experimental spectrum of the underlying molecule.

Our computed spectra for the products of the (*E,E,Z,E*) precursor are presented in Figure 8 for TS1 and in Figure 9 for TS2. In each case, we give the complete spectrum on the left-hand side, while the signals that are observed in the measured spectrum of the synthesized compound are faded out on the right-hand side (thus, only signals that are clearly not observed

dx.doi.org/10.1021/ja2087097 | *J. Am. Chem.Soc.* 2012, 134, 2154–2160

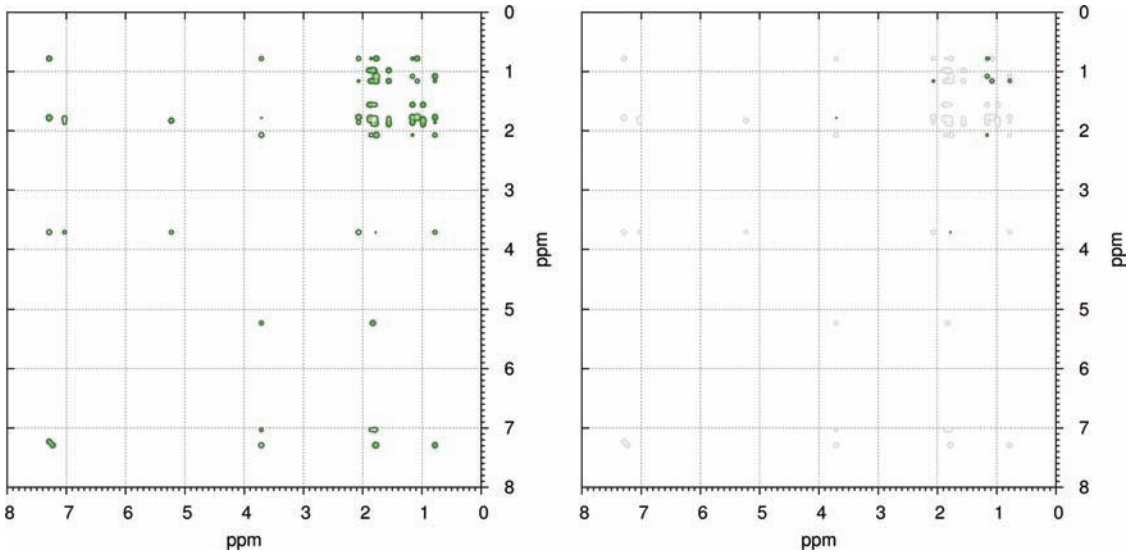

Figure 8. Simulated 2D-NMR spectrum (NOESY) for the product of (*E,E,Z,E*)-TS1 (left). Signals that are present in the experimental spectrum are displayed in light-gray (right).

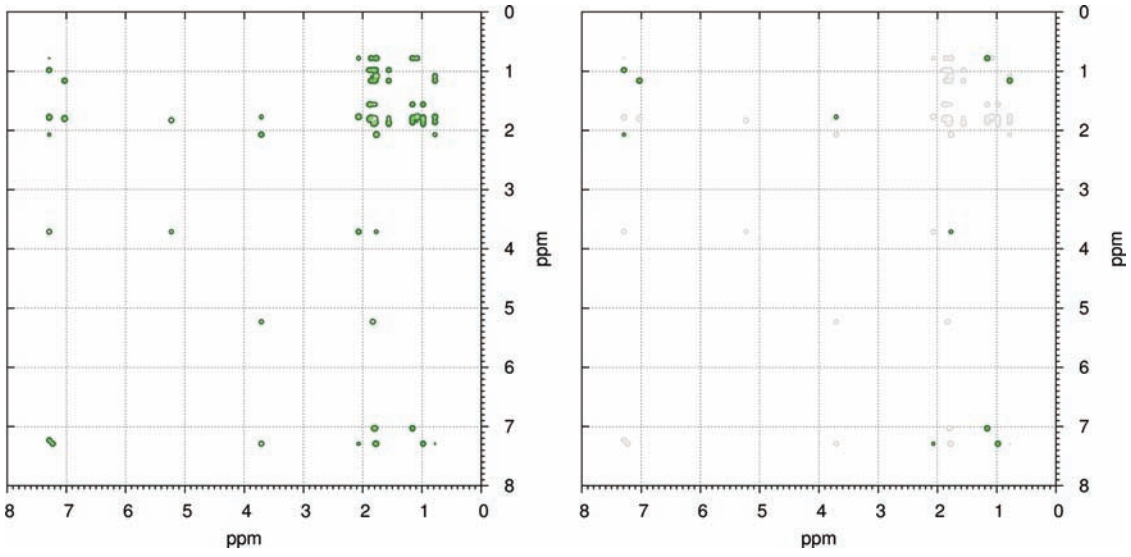

Figure 9. Simulated 2D-NMR spectrum (NOESY) for the product of (*E,E,Z,E*)-TS2 (left). Signals that are present in the experimental spectrum are displayed in light-gray (right).

experimentally remain colored). Comparison of the left- and right-hand sides of Figures 8 and 9 reveals that most of the calculated signals agree with the measured data. However, we also detect signals in both spectra that do not fit the spectrum of the synthesized compound. In the following we focus on signals that are connected with correlations of the stereochemically relevant Me groups (δ = 0.98 ppm and δ = 1.16 ppm, see Figure 10a).

In the simulated spectrum for the product derived from TS2, there are two strong signals at 0.98 ppm/7.29 ppm and 1.16 ppm/7.03 ppm. The corresponding NOESY correlations are illustrated in Figure 10b and concern the Ph group as well as the hydrogen at the double bond. It is obvious that signals due to these correlations can only occur for TS2 but not for TS1. As the signals are not present in the experimental spectrum we safely can rule out that the synthesized structure is the product of (*E,E,Z,E*)-TS2. For the product of TS1 we still find three weak signals that do not agree with the measured data (1.16 ppm/0.78 ppm, 1.16 ppm/1.08 ppm, 1.16 ppm/2.07 ppm). All of them belong to the same Me group. Comparison with the experimental spectrum reveals that these signals appear not at δ = 1.16 ppm but rather at δ = 0.98 ppm. Interchanging the chemical shifts of the corresponding Me groups results in perfect agreement of our calculated and measured data. After interchanging these shifts, all remaining colored signals disappear on the right panel of Figure 8. Thus, also the 2D-NMR spectra suggest that the synthesized molecule is the product of TS1 and not of TS2. We believe that the assignment of the ^{1}H NMR data and the NOESY correlations used in the early work to assess the stereochemistry are the reasons why this original structure determination failed. The previously used correlations are shown in Figure 10c (right) together with the correlations that actually cause the signal (left).

dx.doi.org/10.1021/ja2087097 | *J. Am. Chem.Soc.* 2012, 134, 2154−2160

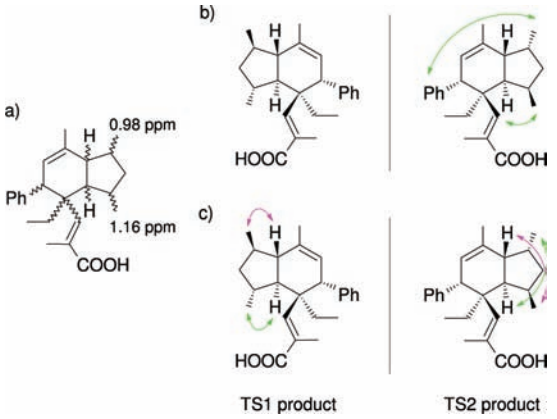

Figure 10. (a) ^{1}H chemical shift of the stereochemically relevant Me groups as assigned previously[1,9] and used for the simulations of the 2D-NMR spectra. (b) NOESY correlations of the strong signals that occur only for the product derived from TS2. (c) Previously used incorrect correlations to derive the structure of plakotenin (right) and correct correlations that actually cause the signals (left).

CONCLUSIONS

In this study, we have addressed the intramolecular Diels–Alder reaction in the total synthesis of plakotenin, a cytotoxic carboxylic acid. The reaction represents a key step because it creates the required carbon framework and stereogenic centers. In view of a potential use for therapy, an efficient synthesis of plakotenin and related compounds is highly desirable. The stereoselectivity of the intramolecular Diels–Alder reaction is therefore of particular interest.

We have examined the product distribution of the reaction through computation of the four possible transition states TS1, TS2, TS3, and TS4 of the tetraene precursor. The (*E,E,Z,E*) configured tetraene that is needed for the synthesis of plakotenin as well as the (*E,E,E,E*) configured tetraene that may be used to access *iso*-plakotenin, a diastereomer of plakotenin, have been considered. On the basis of the relative energies, we have identified TS1 to be the energetically most favored transition state for both precursor molecules. Comparison with the synthesized compounds has revealed that the experimentally assigned structure for *iso*-plakotenin is in agreement with the calculated energies. In the case of plakotenin however, the experimental and computational data at first glance seemed to disagree as the assigned structure would have resulted from TS2, the least favored transition state. Since the properties of synthetic and natural plakotenin are identical, the originally proposed structure must be wrong.

Realizing that crucial parts of the two product structures in question are in an enantiomeric relationship, we have investigated their chiroptical properties. The computed CD spectra and values for optical rotation have allowed a completely conclusive assignment of the synthetic compounds. The products of both the (*E,E,Z,E*)- and (*E,E,E,E*)-tetraene are derived from an intramolecular Diels–Alder reaction via TS1. Thus, the proposed structure of *iso*-plakotenin has proved to be correct, but the structure of plakotenin had to be revised (Figure 11). As the stereochemical assignment of the related compounds *homo*- and *nor*-plakotenin[2] relied on comparison with the structure for plakotenin, the structure of these molecules has to be revised as well (Figure 11).

The present work shows how the interplay between experiment (total synthesis) and theory (computation of reaction barrier heights, chiroptical properties, and 2D-NMR spectra) can help to reveal the absolute stereochemistry of complex organic structures. The computation of reaction barrier heights and the simulation of 2D-NMR spectra, in particular, have proven to be valuable tools.

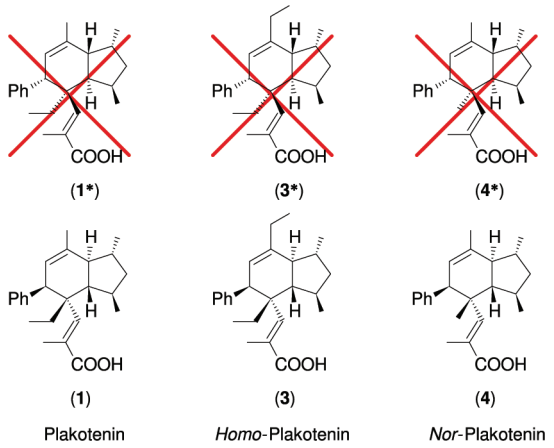

Figure 11. Previously proposed (top) and revised (bottom) structures of plakotenin, *homo*-plakotenin, and *nor*-plakotenin.

EXPERIMENTAL DETAILS

The ^{1}H NMR and two-dimensional NOESY spectra of synthetic plakotenin using $CDCl_3$ as solvent had been published in previous work.[9] Chemical shifts δ are expressed in parts per million (ppm) downfield from tetramethylsilane (TMS) and are referenced to chloroform ($CHCl_3$, δ = 7.26 ppm) as internal standard.

The optical rotations of the products were measured in solution ($CHCl_3$) at 293 K using a Perkin-Elmer 241 polarimeter (Na D-line, 589 nm) and a tempered glass cell of 10-cm length.

All CD measurements were performed using a JASCO J-815-150S CD spectrometer. Solutions of the products (0.1 mg/mL in trifluoroethanol) were prepared and transferred in a 1-mm thick quartz cell. All CD spectra were measured at 293 K.

COMPUTATIONAL DETAILS

All quantum chemical calculations in this work were carried out with the TURBOMOLE program package[10] using standard orbital basis sets (of type "def2", cf. ref 11).

Transition state structures for the various intramolecular Diels–Alder reactions were optimized using the B3LYP hybrid functional[12] in combination with a TZVP basis set and employing tight convergence criteria (SCF energy: 10^{-8} E_h, energy gradient: 10^{-4} $E_h a_0^{-1}$ and inclusion of the derivatives of quadrature weights). Force constants and vibrational frequencies were computed in order to ensure that all structures are first order saddle points with the desired imaginary mode. The reported relative energies are zero point vibrational energy (ZPVE) corrected. For comparison, the transition state structures were also optimized at the BP86[13−15]/SV(P), B3LYP/SV(P), and TPSS[16]/TZVP levels. Furthermore, single-point energy calculations (at the B3LYP/TZVP structures) were performed at the PBE0[17,18]/TZVP and SCS-MP2[19]/TZVPP levels of computation. All of these calculations yield results that are in excellent mutual agreement. For more information, see pp S5–S7 of the Supporting Information.

Optimizations of the multitude of product structures were performed with the TPSS functional using the efficient resolution of the identity (RI approximation) for Coulombic integrals and the smaller SVP basis set.[11] We employed fine quadrature grids (m4),[20] tight convergence criteria (SCF energy: 10^{-8} E_h, energy gradient: 10^{-4} $E_h a_0^{-1}$ and inclusion of the derivatives of quadrature weights) and used the continuum solvent model COSMO[21] to account for solvent effects (ε = 26.7 for trifluoroethanol and ε = 4.8 for chloroform). All structures were confirmed to be minima on the potential energy

dx.doi.org/10.1021/ja2087097 | J. Am. Chem.Soc. 2012, 134, 2154–2160

surface through analysis of force constants and vibrational frequencies. Boltzmann averages of properties were taken on the basis of the ZPVE-corrected relative energies for 293 K (CD, OR) or 298 K (2D-NMR).

Excitation energies and rotatory strengths for CD spectra were computed within the framework of TDDFT response theory[22,23] using the B3LYP functional with diffuse augmented basis sets designed for molecular response calculations (SVPD[24]). CD spectra were simulated by Gaussian broadening (empirical line width: 0.20 eV) and superposition of the computed rotatory strengths. The CD spectra simulated from rotatory-strength values obtained from using the velocity form on the one hand, and the length form on the other hand, mutually agree to within 5%.

Optical rotations were computed within TDDFT response theory[25] using the B3LYP functional and diffuse augmented basis sets (SVPD).

Approximate intensities for 2D-NMR spectra were obtained by considering the distance dependence of the dipolar coupling (intensities are proportional to $1/r^6$), which is the main relaxation effect in nuclear Overhauser enhancement spectroscopy (NOESY). Two-dimensional NMR spectra were simulated by 2D Gaussian broadening (standard deviation: σ = 0.1 ppm) and superposition of intensities $I_{ij} = 1/r_{ij}^6$ for atoms i and j, and by using the experimental ^{1}H NMR chemical shifts.[9] Contour lines are plotted for the intensity values of 0.5 (dark green) and 2.5 (light green).

■ ASSOCIATED CONTENT

Supporting Information

Computed Cartesian atomic coordinates of both considered (*E,E,E,E*) and (*E,E,Z,E*) precursor molecules, computed Cartesian atomic coordinates of all considered (*E,E,E,E*) and (*E,E,Z,E*) transition state conformers, computed Cartesian atomic coordinates of all considered (*E,E,E,E*) and (*E,E,Z,E*) product conformers and relative as well as absolute barrier heights for the intramolecular Diels–Alder reaction. This material is available free of charge via the Internet at http://pubs.acs.org.

■ AUTHOR INFORMATION

Corresponding Author

angela.bihlmeier@kit.edu; klopper@kit.edu

■ ACKNOWLEDGMENTS

We thank Robert Send and Filipp Furche for valuable discussions regarding the TDDFT calculations and the simulation of the CD spectra. Financial support by the Deutsche Forschungsgemeinschaft through the Center for Functional Nanostructures (CFN) in Karlsruhe (Project C3.3) is gratefully acknowledged.

■ REFERENCES

(1) Kobayashi, J.; Takeuchi, S.; Ishibashi, M.; Shigemori, H.; Sasaki, T. *Tetrahedron Lett.* **1992**, *33*, 2579–2580.
(2) Qureshi, A.; Stevenson, C. S.; Albert, C. L.; Jacobs, R. S.; Faulkner, D. J. *J. Nat. Prod.* **1999**, *62*, 1205–1207.
(3) Kirkham, J. E. D.; Lee, V.; Baldwin, J. E. *Chem. Commun.* **2006**, 2863–2865.
(4) Mehta, G.; Kundu, U. K. *Org. Lett.* **2005**, *7*, 5569–5572.
(5) Kirkham, J. E. D.; Lee, V.; Baldwin, J. E. *Org. Lett.* **2006**, *8*, 5537–5540.
(6) Crossman, J. S.; Perkins, M. V. *Tetrahedron* **2008**, 4852–4867.
(7) Matsumura, D.; Toda, T.; Hayamizu, T.; Sawamura, K.; Takao, K.; Tadano, K. *Tetrahedron Lett.* **2009**, 3356–3358.
(8) Huang, X.-H.; van Soest, R.; Roberge, M.; Andersen, R. J. *Org. Lett.* **2004**, 75–78.
(9) Arzt, S.; Bourcet, E.; Muller, T.; Bräse, S. *Org. Biomol. Chem.* **2010**, *8*, 3300–3306.
(10) Program Package for *ab initio* Electronic Structure Calculations, a development of University of Karlsruhe and Forschungszentrum Karlsruhe GmbH. TURBOMOLE, Version 6.1–6.3; University of Karlsruhe and Forschungszentrum Karlsruhe GmbH (Turbomole GmbH since 2007): Karlsruhe, 1989–2007; http://www.turbomole.com.
(11) Weigend, F.; Ahlrichs, R. *Phys. Chem. Chem. Phys.* **2005**, *7*, 3297–3305.
(12) Becke, A. D. *J. Chem. Phys.* **1993**, *98*, 5648–5652.
(13) Vosko, S. H.; Wilk, L.; Nusair, M. *Can. J. Phys.* **1980**, *58*, 1200–1211.
(14) Perdew, J. P. *Phys. Rev. B* **1986**, *33*, 8822–8824.
(15) Becke, A. D. *Phys. Rev. A* **1988**, *38*, 3098–3100.
(16) Tao, J.; Perdew, J. P.; Staroverov, V. N.; Scuseria, G. E. *Phys. Rev. Lett.* **2003**, *91*, 146401.
(17) Perdew, J. P.; Burke, K.; Ernzerhof, M. *Phys. Rev. Lett.* **1996**, *77*, 3865–3868.
(18) Adamo, C.; Barone, V. *Chem. Phys. Lett.* **1998**, *298*, 113–119.
(19) Grimme, S. *J. Chem. Phys.* **2003**, *118*, 9095–9102.
(20) Treutler, O.; Ahlrichs, R. *J. Chem. Phys.* **1995**, *102*, 346–354.
(21) Klamt, A.; Schüürmann, G. *J. Chem. Soc., Perkin Trans. 2* **1993**, 99–805.
(22) Bauernschmitt, R.; Ahlrichs, R. *Chem. Phys. Lett.* **1996**, *256*, 454–464.
(23) Furche, F.; Rappoport, D., III. Density Functional Methods for Excited States: Equilibrium Structure and Electronic Spectra. In *Computational Photochemistry*; Olivucci, M., Ed.; Elsevier: Dordrecht, 2005; Vol. *16*.
(24) Rappoport, D.; Furche, F. *J. Chem. Phys.* **2010**, *133*, 134105.
(25) Grimme, S.; Furche, F.; Ahlrichs, R. *Chem. Phys. Lett.* **2002**, *361*, 321–328.